Sorafenib-Induced Ferroptosis via SLC7A11 Suppression in Triple-Negative Breast Cancer Cells: A Combined Bioinformatics and In Vitro Experimental Evidence

Arya Satya Rajanagara[1]*
[1]*Graduate Institute of Biomedical Sciences, China Medical University, Taichung, Taiwan*

ABSTRACT

Background: Ferroptosis has emerged as a promising anticancer strategy because many tumors develop resistance to apoptosis-based therapies, whereas ferroptosis eliminates cancer cells through a distinct iron-dependent mechanism characterized by lipid peroxidation. *SLC7A11*, a key regulator protein of ferroptosis resistance, is frequently dysregulated in tumors. This study evaluated the clinical relevance of *SLC7A11* in breast cancer and investigated the ferroptosis-inducing potential of sorafenib. **Methods:** TCGA datasets were analyzed through UALCAN Platform to assess *SLC7A11* expression and prognostic significance in breast cancer (BRCA), cervical squamous cell carcinoma (CESC), and head and neck squamous cell carcinoma (HNSC). Expression across breast cancer subtypes and patient survival were examined. *MDA-MB-231* triple-negative breast cancer cells were treated with sorafenib, and changes in morphology, viability, and lipid peroxidation were assessed using microscopy, viability assays, and *C11-BODIPY* flow cytometry assay. **Results:** *SLC7A11* expression was significantly elevated in BRCA, CESC, and HNSC tumors compared with normal tissues (all $p < 0.001$). Within breast cancer, expression was highest in the triple-negative subtype and was associated with poorer overall survival ($p = 0.0065$). Sorafenib significantly reduced *MDA-MB-231* cell viability ($p = 0.0021$) and induced morphological changes consistent with cell damage. *C11-BODIPY* analysis demonstrated increased lipid peroxidation following sorafenib treatment. **Conclusions:** Elevated *SLC7A11* is associated with aggressive breast cancer and poor prognosis. Sorafenib reduces breast cancer cell viability and promotes lipid peroxidation, supporting ferroptosis induction as a potential anticancer mechanism.

ABSTRAK

Latar Belakang: *Ferroptosis menjadi strategi antikanker yang menjanjikan karena banyak tumor resisten terhadap terapi berbasis apoptosis, sementara ferroptosis menargetkan sel kanker melalui mekanisme jalur berbeda yang bergantung pada besi dan ditandai dengan peroksidasi lipid. SLC7A11, protein regulator utama resistensi ferroptosis, sering mengalami peningkatan pada tumor. Penelitian ini mengevaluasi relevansi klinis SLC7A11 pada kanker payudara dan menginvestigasi potensi induksi ferroptosis dengan sorafenib.* ***Metode:*** *Dataset TCGA dianalisis dari UALCAN untuk menilai ekspresi SLC7A11 dan signifikansi prognostiknya pada kanker payudara, kanker sel skuamosa serviks, dan kanker sel skuamosa kepala-leher. Ekspresi antarsubtipe kanker payudara dan kelangsungan hidup pasien turut dievaluasi. Sel MDA-MB-231 diberi perlakuan sorafenib, kemudian dinilai perubahan morfologi, viabilitas, dan peroksidasi lipid menggunakan mikroskop, uji viabilitas, serta flow cytometry C11-BODIPY.* ***Hasil:*** *Ekspresi SLC7A11 secara signifikan lebih tinggi pada tumor (BRCA, CESC, dan HNSC) dibandingkan dengan jaringan normal ($p < 0,001$). Pada kanker payudara, ekspresi tertinggi ditemukan pada subtipe triple-negative dan berhubungan dengan kelangsungan hidup yang lebih buruk ($p = 0,0065$). Sorafenib secara signifikan menurunkan viabilitas sel MDA-MB-231 ($p = 0,0021$) disertai perubahan morfologi yang konsisten dengan kerusakan sel. Analisis C11-BODIPY mengkonfirmasi peningkatan peroksidasi lipid setelah pemberian sorafenib.* ***Kesimpulan:*** *Peningkatan ekspresi SLC7A11 berkaitan dengan kanker payudara yang agresif dan prognosis buruk. Sorafenib terbukti menurunkan viabilitas sel dan memicu peroksidasi lipid, mendukung induksi ferroptosis sebagai mekanisme antikanker yang potensial.*

CONTACT
arya.rajanagara01@gmail.com

KEYWORDS
Breast Cancer, Ferroptosis, Sorafenib

INTRODUCTION

Breast cancer remains the most frequently diagnosed malignancy and a leading cause of cancer-related mortality among women worldwide. Among its molecular subtypes, triple-negative breast cancer (TNBC) defined by the absence of estrogen receptor, progesterone receptor, and HER2 amplification, accounts for a disproportionate share of breast cancer deaths despite representing only 10-15% of diagnoses. The absence of actionable hormonal or HER2-directed targets restricts TNBC treatment largely to cytotoxic chemotherapy, and acquired or intrinsic resistance to apoptosis-inducing agents remains a central obstacle to durable disease control (Bardia et al., 2021). This therapeutic gap has intensified interest in non-apoptotic cell death mechanisms, particularly ferroptosis, as alternative or complementary strategies for TNBC management.

Ferroptosis is an iron-dependent form of regulated cell death driven by the accumulation of lipid peroxides on polyunsaturated fatty acid containing phospholipids, ultimately leading to catastrophic membrane damage (Dixon et al., 2012). Because ferroptosis is mechanistically and genetically distinct from apoptosis, cancer cells that have evolved resistance to apoptotic stimuli may nonetheless remain vulnerable to ferroptosis induction, positioning this pathway as an attractive therapeutic avenue in treatment-refractory tumors such as TNBC (Jiang et al., 2015). Central to ferroptosis resistance is the cystine/glutamate antiporter system xc^-, whose functional subunit SLC7A11 (also known as xCT) mediates cellular uptake of cystine in exchange for glutamate. Cystine imported via SLC7A11 is reduced intracellularly to cysteine, the rate-limiting substrate for glutathione (GSH) biosynthesis. GSH, in turn, is required as a cofactor for glutathione peroxidase 4 (GPX4), the principal enzyme responsible for detoxifying lipid peroxides and thereby restraining ferroptotic cell death (Yang et al., 2014). Overexpression of SLC7A11 has been reported across multiple malignancies, where it sustains an antioxidant reserve that protects tumor cells from oxidative and ferroptotic insults, and has been linked to more aggressive disease phenotypes and inferior clinical outcomes (Koppula et al., 2021). Sorafenib, a multikinase inhibitor originally developed and approved for hepatocellular carcinoma and renal cell carcinoma, has been shown in several preclinical settings to suppress system xc^- activity and deplete intracellular glutathione, thereby sensitizing cells to ferroptotic death independent of its canonical antiangiogenic and antiproliferative kinase-inhibitory actions (Dixon et al., 2014; Louandre et al., 2013). This repurposing potential is of particular interest for TNBC, where few targeted options exist.

Despite accumulating evidence implicating SLC7A11 in ferroptosis resistance across cancer types, the clinical relevance of SLC7A11 expression specifically within breast cancer molecular subtypes, and its association with patient survival, has not been comprehensively characterized alongside functional validation of ferroptosis induction in a TNBC cell model. In this study, we combined bioinformatic analysis of The Cancer Genome Atlas (TCGA) with in vitro experimentation to (1) characterize SLC7A11 expression across breast cancer, cervical squamous cell carcinoma, and head and neck squamous cell carcinoma relative to normal tissue; (2) determine whether SLC7A11 expression differs across breast cancer molecular subtypes and correlates with overall survival; and (3) evaluate whether sorafenib induces ferroptotic features reduced viability, morphological damage, and lipid peroxidation in MDA-MB-231 TNBC cells. We hypothesized that SLC7A11 overexpression marks a more aggressive, ferroptosis-resistant breast cancer phenotype that can nonetheless be therapeutically exploited through sorafenib-induced ferroptosis.

MATERIALS AND METHODS

Bioinformatic analysis of SLC7A11 expression using TCGA data

SLC7A11 mRNA expression was examined using the UALCAN web portal (*https://ualcan.path.uab.edu/*), which provides interactive access to processed TCGA RNA-sequencing data (Chandrashekar, 2017). Transcript-per-million (TPM) values for SLC7A11 were compared between primary tumor and normal tissue samples in three TCGA cohorts: breast invasive carcinoma (BRCA; normal n = 114, primary tumor n = 1097), cervical squamous cell carcinoma (CESC; normal n = 3, primary tumor n = 305), and head and neck squamous cell carcinoma (HNSC; normal n = 44, primary tumor n = 520). For BRCA, SLC7A11 expression was additionally stratified by molecular subtype (normal-adjacent, luminal, HER2-positive, and triple-negative) based on UALCAN's PAM50/clinical subtype classification. Between-group comparisons were performed using the built-in statistical framework of UALCAN, which applies a student's t-test to compare expression distributions between groups.

Survival analysis

The prognostic significance of SLC7A11 expression in breast cancer was assessed using UALCAN's survival analysis module, which stratifies TCGA-BRCA patients into high-expression (n = 271) and low/medium-expression (n = 810) groups based on SLC7A11 transcript levels, using an optimal or median expression cutoff. Kaplan-Meier survival curves were generated, and differences in overall survival between groups were evaluated using the log-rank test.

Cell culture

The MDA-MB-231 triple-negative breast cancer cell line was cultured in Dulbecco's Modified Eagle Medium (DMEM) supplemented with 10% fetal bovine serum (FBS) and 1% penicillin-streptomycin, and maintained at 37°C in a humidified incubator with 5% CO_2. Cells were passaged upon reaching 70-80% confluence and used within a limited passage range to minimize phenotypic drift.

Sorafenib treatment

MDA-MB-231 cells were seeded and allowed to adhere for 24 hours prior to treatment. Cells were subsequently treated with sorafenib (10 μM) or vehicle control (dimethyl sulfoxide, DMSO, at an equivalent final concentration) for 24 hours. Cell morphology was assessed by bright-field microscopy prior to downstream viability and lipid peroxidation assays.

Cell viability assay

Cell viability following sorafenib treatment was quantified using a colorimetric viability assay. Following 24 hours of treatment, cell viability was expressed as a percentage relative to vehicle-treated controls. Each condition was performed in triplicate, and results are presented as mean ± standard deviation (SD). Statistical comparison between control and sorafenib-treated groups was performed using an unpaired two-tailed Student's t-test, with $p < 0.05$ considered statistically significant.

Lipid peroxidation assay (C11-BODIPY flow cytometry)

Lipid peroxidation was assessed using the ratiometric fluorescent probe C11-BODIPY(581/591). Following treatment, cells were incubated with C11-BODIPY, harvested, and analyzed by flow cytometry. Upon oxidation, the probe undergoes a shift in fluorescence emission from red (non-oxidized, PE-A channel) to green (oxidized, FITC-A channel), and the resulting FITC-A/PE-A ratio was used to quantify the degree of lipid peroxidation, with a rightward shift in the histogram indicating increased oxidative lipid damage relative to vehicle-treated control cells.

Statistical analysis

All in vitro experiments were performed in at least three independent replicates unless otherwise stated. Data are presented as mean ± SD. Comparisons between two groups were performed using an unpaired two-tailed Student's t-test. For bioinformatic analyses, statistical comparisons were generated within the UALCAN platform. A p-value < 0.05 was considered statistically significant (*$p < 0.05$, **$p < 0.01$, ***$p < 0.001$).

RESULTS

SLC7A11 is significantly overexpressed in BRCA, CESC, and HNSC tumors relative to normal tissue

To evaluate the clinical relevance of SLC7A11 across malignancies with documented ferroptosis-resistance phenotypes, we first compared SLC7A11 transcript expression between tumor and normal tissue using TCGA data. In the BRCA cohort, SLC7A11 expression was markedly higher in primary tumors (n = 1097) than in normal breast tissue (n = 114; $p = 2.25 \times 10^{-12}$; Figure 1A). A similar pattern was observed in CESC, where primary tumor samples (n = 305) showed significantly elevated SLC7A11 expression compared with normal cervical tissue (n = 3; $p = 4.51 \times 10^{-9}$; Figure 1A). In HNSC, SLC7A11 expression was likewise significantly increased in primary tumors (n = 520) relative to normal tissue (n = 44; $p = 1.22 \times 10^{-15}$; Figure 1A). Together, these findings indicate

that SLC7A11 upregulation is a consistent feature across squamous and breast malignancies, supporting its candidacy as a broadly relevant marker of ferroptosis resistance.

SLC7A11 expression is highest in the triple-negative breast cancer subtype

Given the well-documented molecular heterogeneity of breast cancer, we next examined whether SLC7A11 expression differed across breast cancer molecular subtypes. Stratification of TCGA-BRCA samples by subtype revealed that SLC7A11 expression progressively increased from normal tissue (n = 114) to luminal (n = 566) and HER2-positive (n = 37) tumors, reaching its highest level in the triple-negative subtype (n = 116; Figure 1B). This subtype-specific enrichment suggests that SLC7A11-driven ferroptosis resistance may be particularly pronounced in TNBC, the subtype with the fewest targeted treatment options.

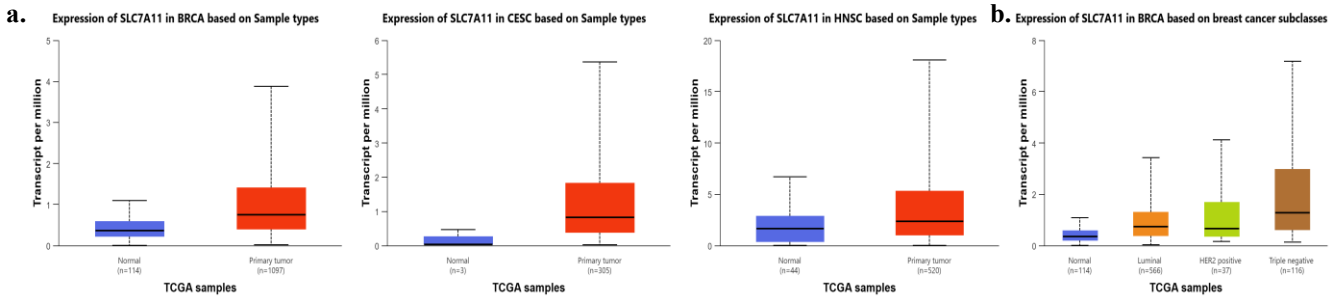


Figure 1. *SLC7A11 expression across TCGA tumor cohorts and breast cancer molecular subtypes. (A) SLC7A11 transcript expression (transcripts per million) in normal versus primary tumor tissue for breast invasive carcinoma (BRCA), CESC, HNSC. (B) SLC7A11 expression across BRCA molecular subtypes (normal, luminal, HER2-positive, triple-negative). Data are presented as box-and-whisker plots; p-values were generated within the UALCAN platform. Source: UALCAN (https://ualcan.path.uab.edu/).*

High SLC7A11 expression is associated with poorer overall survival in breast cancer

To determine whether elevated SLC7A11 expression carries prognostic significance, Kaplan-Meier survival analysis was performed comparing BRCA patients with high (n = 271) versus low/medium (n = 810) SLC7A11 expression. Patients with high SLC7A11 expression exhibited significantly reduced overall survival compared with those with low/medium expression (p = 0.0065; Figure 2). This finding is consistent with a model in which SLC7A11-mediated cystine uptake and glutathione synthesis confer a survival advantage to breast tumor cells by suppressing ferroptotic vulnerability, thereby contributing to more aggressive disease behavior.

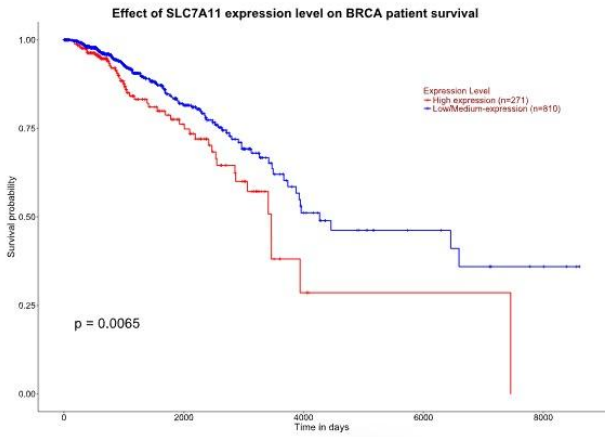


Figure 2. *SLC7A11 expression and overall survival in breast cancer. Kaplan-Meier overall survival curve for TCGA-BRCA patients stratified by high (n = 271) versus low/medium (n = 810) SLC7A11 expression. Statistical significance was assessed using the log-rank test (p = 0.0065). Source: UALCAN (https://ualcan.path.uab.edu/).*

Sorafenib induces morphological changes consistent with cell damage in MDA-MB-231 cells

Given the elevated SLC7A11 expression and adverse prognosis observed in TNBC, we next tested whether pharmacological induction of ferroptosis could be achieved in an experimental TNBC model. MDA-MB-231 cells treated with sorafenib (10 μM, 24 hours) displayed marked morphological alterations relative to vehicle-treated controls, including cell shrinkage, rounding, loss of the characteristic spindle-shaped morphology, and reduced cell density (Figure 3A), consistent with treatment-induced cytotoxic stress.

Sorafenib significantly reduces MDA-MB-231 cell viability

Quantitative viability assessment confirmed the morphological findings: sorafenib treatment significantly reduced MDA-MB-231 cell viability compared with vehicle-treated controls (approximately 88% viability in control versus approximately 46% in sorafenib-treated cells; $p = 0.0021$; Figure 3B), corresponding to an approximately 47% reduction in viable cells following 24 hours of sorafenib exposure.

Sorafenib increases lipid peroxidation in MDA-MB-231 cells

To determine whether the observed reduction in viability was accompanied by ferroptosis-associated lipid peroxidation, C11-BODIPY flow cytometry was performed. Control cells displayed a predominant peak in the non-oxidized (reduced) fluorescence channel. Following sorafenib treatment (10 μM, 24 hours), a pronounced rightward shift in the fluorescence histogram was observed, indicating a substantial increase in the oxidized probe fraction and, correspondingly, elevated lipid peroxidation (Figure 3C). This shift provides direct experimental evidence that sorafenib promotes lipid peroxidation in MDA-MB-231 cells, consistent with induction of ferroptosis.

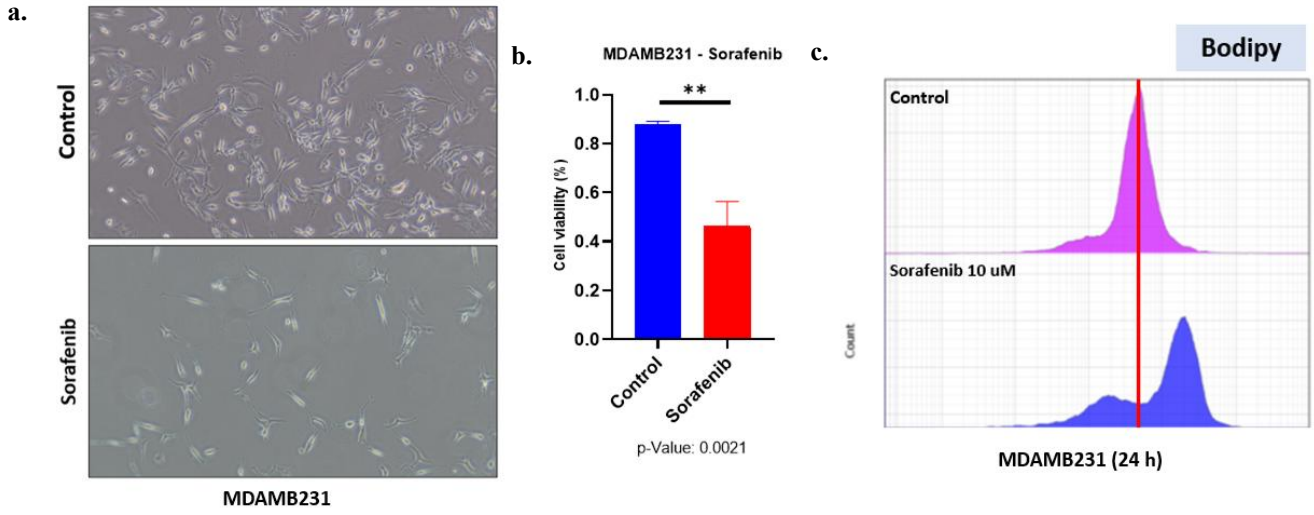


Figure 3. *Sorafenib reduces cell viability and induces lipid peroxidation in MDA-MB-231 triple-negative breast cancer cells. (A) Representative bright-field micrographs of MDA-MB-231 cells following vehicle (control) or sorafenib (10 μM, 24 h) treatment. (B) Cell viability of MDA-MB-231 cells treated with vehicle or sorafenib (10 μM, 24 h), expressed as percentage viability (mean ± SD; **$p < 0.01$, unpaired two-tailed Student's t-test; $p = 0.0021$). (C) C11-BODIPY flow cytometry histograms showing oxidized-probe fluorescence in control versus sorafenib-treated (10 μM, 24 h) MDA-MB-231 cells; the rightward shift indicates increased lipid peroxidation following sorafenib exposure.*

DISCUSSION

This study integrated TCGA-based bioinformatic analysis with in vitro experimentation to characterize the role of SLC7A11 in breast cancer and to evaluate sorafenib as a ferroptosis-inducing agent in TNBC. We found that SLC7A11 is significantly overexpressed in BRCA, CESC, and HNSC tumors relative to normal tissue, that its expression is highest within the triple-negative breast cancer subtype, and that elevated expression is associated with significantly worse overall survival. Functionally, sorafenib treatment of MDA-MB-231 cells produced morphological changes consistent with cell damage, significantly reduced cell viability, and increased lipid peroxidation, together supporting ferroptosis induction as a contributing mechanism of sorafenib's cytotoxic effect in this TNBC model. The consistent overexpression of SLC7A11 across three histologically distinct tumor types

is in line with a growing body of literature implicating system xc⁻ activity as a common adaptive mechanism by which tumor cells buffer against oxidative and ferroptotic stress (Koppula et al., 2021). Because SLC7A11 sits upstream of glutathione biosynthesis and GPX4-mediated lipid peroxide detoxification, its upregulation may represent a convergent survival strategy exploited by tumors originating from diverse tissue contexts, reinforcing its candidacy as a pan-cancer biomarker of ferroptosis resistance rather than a phenomenon restricted to a single malignancy (Yang et al., 2014).

Within breast cancer, the observation that SLC7A11 expression was highest in the triple-negative subtype is particularly noteworthy given the clinical challenges associated with TNBC management. The absence of hormone receptor and HER2-directed therapeutic targets in TNBC has historically limited treatment to cytotoxic chemotherapy (Bardia et al., 2021), and our finding that SLC7A11 overexpression tracks with this subtype, together with its association with inferior overall survival, suggests that ferroptosis-resistance pathways may contribute meaningfully to the aggressive clinical course characteristic of TNBC. These findings extend prior work linking SLC7A11 to poor prognosis in other cancer types (Lang et al., 2019; Koppula et al., 2021), and provide breast cancer subtype-specific context that has been comparatively underexplored. Mechanistically, our in vitro findings are consistent with reports that sorafenib can suppress system xc⁻ function and lower intracellular glutathione availability, thereby lowering the threshold for lipid peroxide accumulation (Dixon et al., 2014; Louandre et al., 2013), independent of its canonical multikinase-inhibitory activity against RAF, VEGFR, and PDGFR signaling. The pronounced rightward shift in the C11-BODIPY fluorescence histogram following sorafenib treatment provides direct evidence of oxidative lipid damage, while the concurrent loss of viability and morphological deterioration support a model in which ferroptosis contributes, at least in part, to sorafenib-induced cytotoxicity in MDA-MB-231 cells. Because MDA-MB-231 is a well-characterized TNBC line with relatively high basal SLC7A11 expression, these cells may represent a particularly ferroptosis-susceptible model once system xc⁻ activity is pharmacologically inhibited, offering a plausible mechanistic link between our bioinformatic and experimental findings.

These results carry potential therapeutic implications. Given that TNBC frequently exhibits reduced sensitivity to apoptosis-inducing chemotherapy (Bardia et al., 2021), agents capable of engaging non-apoptotic death pathways such as ferroptosis may offer a complementary or alternative therapeutic strategy, particularly in tumors with high SLC7A11 expression that might otherwise be expected to resist oxidative challenge. As a clinically approved, repurposable agent, sorafenib's capacity to induce ferroptotic features in TNBC cells strengthens the rationale for further investigation of ferroptosis-inducing strategies whether through sorafenib alone, in combination with other system xc⁻ or GPX4-targeting agents (Yang & Stockwell, 2008; Yang et al., 2014), or as an adjunct to standard chemotherapy in SLC7A11-high TNBC. This study has several limitations. First, the bioinformatic analyses relied on publicly available TCGA transcriptomic data, which reflect bulk tumor expression and cannot resolve cell-type-specific or intratumoral heterogeneity in SLC7A11 expression. Second, the in vitro experiments were performed in a single TNBC cell line (MDA-MB-231); validation across additional TNBC and non-TNBC cell lines, as well as normal mammary epithelial controls, is needed to confirm the generalizability and selectivity of sorafenib-induced ferroptosis. Third, while the C11-BODIPY assay and viability data support ferroptosis induction, definitive confirmation would benefit from additional mechanistic evidence, including rescue experiments using ferroptosis inhibitors (e.g., ferrostatin-1, liproxstatin-1) or iron chelators (e.g., deferoxamine), direct quantification of malondialdehyde or 4-hydroxynonenal as lipid peroxidation end-products, and assessment of downstream effectors such as GPX4 protein expression and glutathione levels following sorafenib exposure. Finally, survival analyses were derived from retrospective TCGA cohorts and should be interpreted as hypothesis-generating rather than causally definitive, given the potential influence of unmeasured clinical covariates.

Future studies should address these limitations through mechanistic rescue experiments to confirm the ferroptotic nature of sorafenib-induced cell death, extension to additional TNBC models and patient-derived xenografts, and evaluation of combinatorial strategies pairing sorafenib with established ferroptosis inducers or standard-of-care chemotherapeutics. Investigation of the transcriptional and epigenetic regulators governing SLC7A11 overexpression in TNBC including possible interplay with stress-responsive transcription factors implicated in ferroptosis resistance, may further clarify the upstream drivers of this phenotype and identify additional therapeutic vulnerabilities.

CONCLUSIONS

SLC7A11 is significantly overexpressed in breast, cervical, and head and neck squamous cell carcinomas relative to normal tissue, with expression highest in the triple-negative breast cancer subtype and associated with significantly poorer overall survival. Sorafenib treatment of MDA-MB-231 TNBC cells induced morphological damage, significantly reduced cell viability, and increased lipid peroxidation, collectively supporting ferroptosis induction as a contributing mechanism of sorafenib cytotoxicity. These findings position SLC7A11 as a clinically relevant marker of ferroptosis resistance in breast cancer and support further investigation of sorafenib and other system xc^--targeting strategies as potential therapeutic approaches for SLC7A11-high triple-negative breast cancer.

DATA AVAILABLE STATEMENT

Publicly available TCGA datasets analyzed in this study can be accessed through the UALCAN platform (*https://ualcan.path.uab.edu/*). Additional experimental data are available from the corresponding author upon reasonable request.

REFERENCES

Bardia, A., Hurvitz, S. A., Tolaney, S. M., Loirat, D., Punie, K., Oliveira, M., Brufsky, A., Sardesai, S. D., Kalinsky, K., Zelnak, A. B., Weaver, R., Traina, T. A., Dalenc, F., Aftimos, P., Lynce, F., Diab, S., Cortes, J., O'Shaughnessy, J., Rugo, H. S., & ASCENT Clinical Trial Investigators. (2021). Sacituzumab govitecan in metastatic triple-negative breast cancer. *New England Journal of Medicine, 384*(16), 1529–1541. https://doi.org/10.1056/NEJMoa2028485

Chandrashekar, D. S., Bashel, B., Balasubramanya, S. A. H., Creighton, C. J., Ponce-Rodriguez, I., Chakravarthi, B., & Varambally, S. (2017). UALCAN: A portal for facilitating tumor subgroup gene expression and survival analyses. *Neoplasia, 19*(8), 649–658. https://doi.org/10.1016/j.neo.2017.05.002

Dixon, S. J., Lemberg, K. M., Lamprecht, M. R., Skouta, R., Zaitsev, E. M., Gleason, C. E., Patel, D. N., Bauer, A. J., Cantley, A. M., Yang, W. S., Morrison, B., & Stockwell, B. R. (2012). Ferroptosis: An iron-dependent form of nonapoptotic cell death. *Cell, 149*(5), 1060–1072. https://doi.org/10.1016/j.cell.2012.03.042

Dixon, S. J., Patel, D. N., Welsch, M., Skouta, R., Lee, E. D., Hayano, M., Thomas, A. G., Gleason, C. E., Tatonetti, N. P., Slusher, B. S., & Stockwell, B. R. (2014). Pharmacological inhibition of cystine-glutamate exchange induces endoplasmic reticulum stress and ferroptosis. *eLife, 3*, e02523. https://doi.org/10.7554/eLife.02523

Jiang, L., Kon, N., Li, T., Wang, S.-J., Su, T., Hibshoosh, H., Baer, R., & Gu, W. (2015). Ferroptosis as a p53-mediated activity during tumour suppression. *Nature, 520*(7545), 57–62. https://doi.org/10.1038/nature14344

Koppula, P., Zhuang, L., & Gan, B. (2021). Cystine transporter SLC7A11/xCT in cancer: Ferroptosis, nutrient dependency, and cancer therapy. *Protein & Cell, 12*(8), 599–620. https://doi.org/10.1007/s13238-020-00789-5

Lang, X., Green, M. D., Wang, W., Yu, J., Choi, J. E., Jiang, L., Liao, P., Zhou, J., Zhang, Q., Dow, A., Saripalli, A., Kryczek, I., Wei, S., Szeliga, W., Vatan, L., Stone, G., Georgiou, G., Huang, L., Zou, W., & Liu, Q. (2019). Radiotherapy and immunotherapy promote tumoral lipid oxidation and ferroptosis via synergistic repression of SLC7A11. *Cancer Discovery, 9*(12), 1673–1685. https://doi.org/10.1158/2159-8290.CD-19-0338

Louandre, C., Ezzoukhry, Z., Godin, C., Barbare, J.-C., Mazière, J.-C., Chauffert, B., Galmiche, A., & Saidak, Z. (2013). Iron-dependent cell death of hepatocellular carcinoma cells exposed to sorafenib. *International Journal of Cancer, 133*(7), 1732–1742. https://doi.org/10.1002/ijc.28159

Yang, W. S., SriRamaratnam, R., Welsch, M. E., Shimada, K., Skouta, R., Viswanathan, V. S., Cheah, J. H., Clemons, P. A., Shamji, A. F., Clish, C. B., Brown, L. M., Girotti, A. W., Cornish, V. W., Schreiber, S. L., & Stockwell, B. R. (2014). Regulation of ferroptotic cancer cell death by GPX4. *Cell, 156*(1–2), 317–331. https://doi.org/10.1016/j.cell.2013.12.010

Yang, W. S., & Stockwell, B. R. (2008). Synthetic lethal screening identifies compounds activating iron-dependent, nonapoptotic cell death in oncogenic RAS-harboring cancer cells. *Chemistry & Biology, 15*(3), 234–245. https://doi.org/10.1016/j.chembiol.2008.02.010